

A Wireless, Low-Drift, Implantable Intraocular Pressure Sensor with Parylene-on-oil Encapsulation

Abhinav Agarwal^{1*}, Aubrey Shapero^{1*}, Damien Rodger², Mark Humayun², Yu-Chong Tai¹, and Azita Emami¹

¹California Institute of Technology, Pasadena, CA, USA

²USC Keck School of Medicine, Los Angeles, CA, USA

Abstract—This paper presents a wireless, implantable continuous intraocular pressure (IOP) monitoring system that features a parylene-on-oil sensor encapsulation method for achieving long-term low-drift *in vivo*. The system is implanted in the superotemporal quadrant of the eye between the sclera and conjunctiva. It consists of a commercial pressure sensor (STMicroelectronics LPS25H) with digital readout, a 65nm CMOS chip that supports wireless power/data telemetry and the I2C serial communication interface with the pressure sensor. The chip and pressure sensor are assembled on a flexible polyimide PCB, and then the sensor is submerged in biocompatible silicone oil and coated with parylene *in situ*. The implant uses an on-chip integrated RF coil to receive power from near-field RF coupling at 915 MHz and transmit measurement bits via RF-backscattering to an external reader. A 2 mm x 1.2 mm chip is fabricated in TSMC 65nm CMOS process. The IOP implant achieves a pressure sensitivity of 0.17 mmHg with a total power consumption of 9.7 μW. We demonstrate pressure offset drift of less than 0.5 mmHg for more than 4 months over a temperature range of 27–38 °C. The implant successfully tracks induced IOP variations in a porcine eye *ex vivo*, validating the system functionality and surgical implantation.

Keywords—Intraocular Pressure Sensor (IOP); Implantable; Parylene-on-oil; Pressure Sensor Packaging; Low-Drift; Wireless Powering; RF Backscattering

I. INTRODUCTION

Glaucoma is the second leading cause of blindness, affecting 60 million people across the globe [1]. A major risk factor for glaucoma is increased intraocular pressure (IOP), which damages the optic nerve and leads to blindness. The current standard of care for monitoring IOP is Goldmann applanation tonometry, in which patients visit the doctor's office regularly to register a single measurement per visit. It is known that IOP fluctuates throughout the day, and infrequent

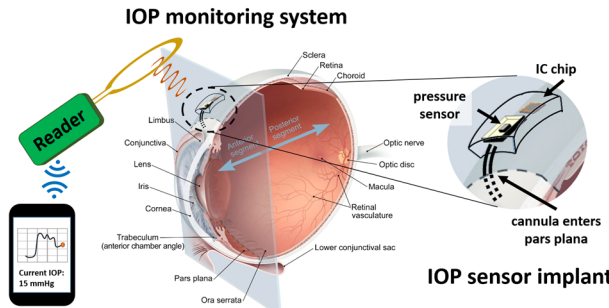


Figure 1: Continuous IOP monitoring system. A wireless reader powers and receives backscattered data from the IC chip and relays it to a mobile device.

measurements can miss elevated IOP spikes, leading to inaccurate assessment [2]. Thus, a continuous, implantable IOP monitor is necessary for an accurate diagnosis, to monitor treatment, and to avoid preventable permanent vision loss.

Due to sensor drift caused by chemo-biological factors such as hydrolytic corrosion and biofouling, no implantable IOP sensor has been shown to maintain a clinical accuracy target of <2 mmHg for more than one month without recalibration [3], which defeats the purpose of continuous monitoring. Such a short lifetime has rightfully prevented the use of IOP monitoring implants [4]. Past efforts have erroneously assumed that the temperature at an IOP sensor implant location is constant, so temperature measurements are ignored. However, temperature dependent effects can be major sources of IOP sensor inaccuracy [5]. In addition, implantable IOP sensors need to have a small and practical form factor, low power consumption, and wireless operation.

We present a wireless, implantable IOP monitor (Fig. 1) capable of sub-mmHg accurate long-term measurements by using a parylene-on-oil pressure sensor encapsulation [6]. The system is implanted in superotemporal quadrant of the eye between the sclera and conjunctiva, where IOP is accessed through a cannula via the pars plana.

II. SYSTEM ARCHITECTURE

The IOP monitoring implant consists of a digital barometer with pressure and temperature readout (ST-Microelectronics LPS25H), decoupling and charge storage capacitors, a custom designed CMOS chip containing the power management circuitry, a data telemetry unit and a serial I2C interface with the sensor (Fig. 2). The components are assembled on a flexible polyimide PCB. The pressure sensor is packaged using a parylene-on-oil method, in which the sensor is submerged in biocompatible silicone oil and then coated with parylene *in situ* using chemical vapor deposition

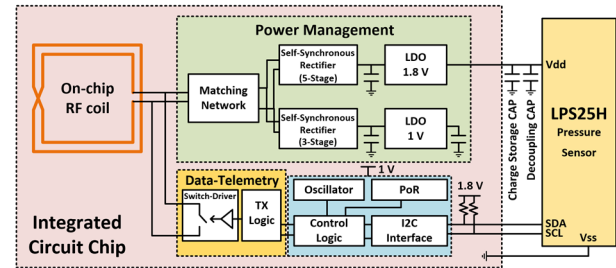


Figure 2: System-level block diagram of IOP monitor

* These authors contributed equally

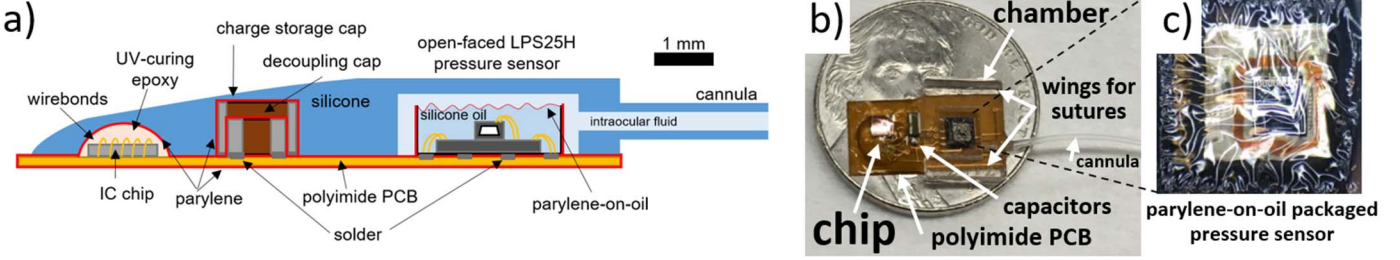


Figure 3: a) Cross-section of the implant. (To-scale, with exception of parylene thickness, which is enlarged for clarity). b) Photo of implant on a US nickel. c) Enlarged image of parylene-on-oil encapsulation on a pressure sensor (LPS25H).

(CVD). A cross-sectional diagram of the implant is shown in Fig. 3a, and a photo is shown in Fig. 3b, with a close-up of the parylene-on-oil encapsulation in Fig. 3c.

A. Integrated Circuit Chip

The CMOS chip receives power from near-field RF coupling to an on-chip integrated coil at 915 MHz, which lies in the ISM band of the EM spectrum (Fig. 4a). The coil is placed in the top metal layer of the process and is optimized to achieve a high quality factor of 20 at 915 MHz (Fig. 4b) to maximize the RF power transfer efficiency. Fig. 4c shows the ANSYS HFSS simulation results of link-loss at a separation of 1cm (5mm air + 5mm tissue) between the external coil and the on-chip integrated coil.

The power management unit consists of a rectifier (Fig. 4d), a bandgap reference and a low-dropout voltage regulator (LDO) (Fig. 4e) which generates a stable supply voltage of 1.8V for the pressure sensor. In addition, the chip has a separate rectifier and an LDO to generate a supply voltage of 1.0V for the digital logic. A self-synchronous rectifier topology [7] is used to rectify low voltage, high frequency differential RF signals at relatively high efficiency.

When RF power is applied for the first time, the chip generates a power-on-reset (PoR) signal, which resets the digital logic on-chip and starts the 1 MHz on-chip relaxation oscillator (Fig. 4f).

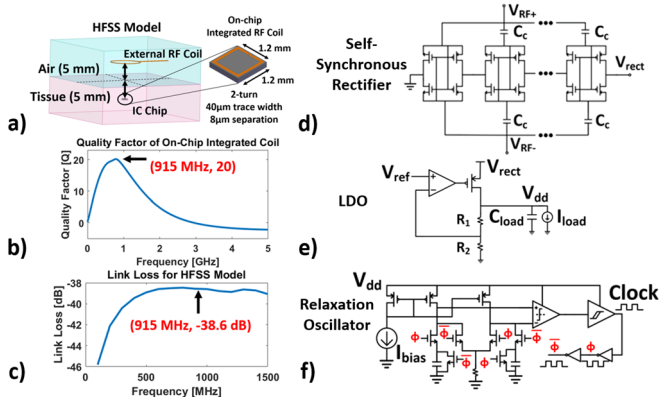


Figure 4: a) HFSS model simulating RF power transfer. b) Quality factor of optimized on-chip integrated coil. c) Link loss for RF power transfer. d) Self-synchronous rectifier topology. e) Low-dropout voltage regulator (LDO) topology. f) Relaxation oscillator topology.

The chip communicates with the pressure sensor over the I2C serial communication protocol. Upon power-on-reset, the digital logic executes a series of pre-programmed commands and delays and receives the output bits from the pressure sensor. Once a second, the chip requests the pressure sensor to make a measurement, waits for the data to be available, and then reads the 24-bit pressure and 16-bit temperature data, as well as a fixed 8-bit identifier address to ensure valid communication. The pressure sensor is highly duty-cycled and returns to sleep mode to save power.

Finally, the data telemetry block collects the 48-bit sample, and wirelessly transmits it to the external reader via PWM backscattering, along with a prefix and suffix for packet identification.

B. Pressure Sensor Packaging and System Assembly

Our system uses the LPS25H, a digital output pressure sensor with internal temperature calibration. It is also low power, $2.5 \times 2.5 \times 0.8 \text{ mm}^3$ in size, requires a minimum supply voltage of 1.7V, and can achieve a pressure resolution of 0.08 mmHg in the lowest power mode. The pressure sensor and capacitors are first soldered onto the flexible polyimide PCB. The IC chip is then epoxied and wirebonded to the PCB. Masterbond UV10TKMed UV-curable epoxy is deposited over the wirebonds to secure them.

Next, the sensor is packaged using the parylene-on-oil method: First, the top of the plastic housing for the LPS25H is removed with a razor blade so that the pressure sensor chamber resides in an open-faced box. Biocompatible, 100,000 cSt silicone oil is deposited onto the sensor. Then, thick parylene-C ($>10\mu\text{m}$) is deposited on the components. Thick parylene induces excessive drift, so the parylene over the pressure sensor is cut with a blade and removed with tweezers. More oil is deposited with a syringe, and a flat edge is used to level the oil inside the plastic housing. A second, sub-micron layer of parylene-C is deposited in high vacuum, encapsulating the silicone oil bubble-free. The silicone oil prevents corrosion because of its low liquid water and water vapor solubility. In contrast, silicone gel has higher water vapor solubility. The silicone oil is deposited before the first parylene deposition to prevent parylene from directly touching the membrane, which would distort the device's sensitivity. Last, a silicone chamber and a flexible 23-gauge silicone tube are adhered to the PCB over the pressure sensor.

III. MEASUREMENT RESULTS

The long-term, low-drift capability of the parylene-on-oil encapsulation method and circuit functionality were first verified independently. Then, the implant was calibrated in air over pressure and temperature variation. The implantation procedure was validated by successfully recording induced IOP variations in a vitrectomized *ex vivo* porcine eye.

A. Long-term, Low-drift Saline Soaking Test

Lifetime soaking tests of wired devices in 0.9% saline, mimicking body fluid, validate the low-drift capability of the packaging method [8]. Parylene-C has a glass transition temperature at 42 °C, so it was soaked at 37 °C. Fig. 5 shows pressure offset relative to a control device versus temperature, at different months. After accounting for temperature dependence from the ‘0 month’ data, there is less than 0.5 mmHg drift over the temperature range of 27–38 °C for over 4 months. Also, a negligible amount of hysteresis is seen. This suggests that stable, temperature-compensated, pre-implantation calibrated values can yield sufficient accuracy for long-term use.

B. Wireless Powering and Data Telemetry

The wireless reader uses a Nordic nRF51 Bluetooth SoC, which controls a UHF RFID chipset (AMS 3993) (Fig. 6a).

The optimum frequency for RF power transfer strongly depends on the medium and separation between the external coil and the implant. Since the separation and biological properties of tissues may vary among individuals, it is necessary to tune the frequency to achieve maximum power transfer efficiency [9]. For this, we implement an auto-tuning algorithm on the Bluetooth SoC, which scans a frequency range and locates the frequency at which the reflected RF power into the UHF RFID chipset is minimized.

Once the optimum frequency is determined, the reader powers up the implant at that frequency (Fig. 6b) and waits to receive the backscattered measurement bits (Fig. 6c).

C. Wireless operation in air.

The parylene-on-oil encapsulation induces small pressure offset. After the implant is assembled, it is baked in 37 °C air overnight to circumvent independent aging effects with short

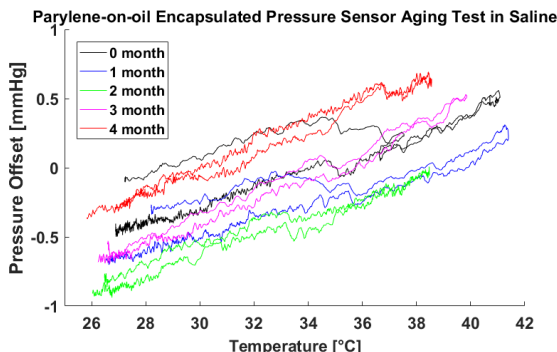


Figure 5: Parylene-on-oil encapsulated pressure sensor offset drift measurements. The sensor is stored in 0.9% saline at 37 °C (700nm-thick parylene-C). In four months, pressure offset drifted less than 0.5 mmHg over 27–38 °C, compared to ‘0 month’.

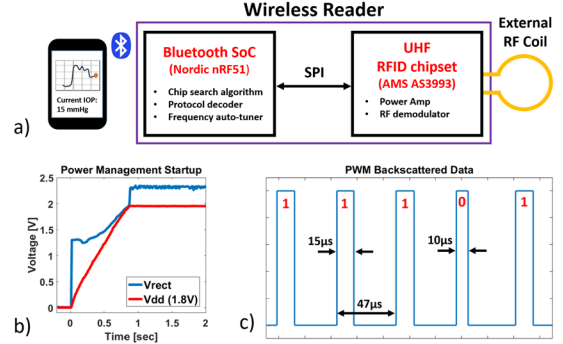


Figure 6: a) Wireless reader system b) Startup of power management circuitry upon RF powering. c) PWM backscattered ‘11101’ data fragment digitized by UHF RFID chipset

time-constants. At this point, the offset has a stable temperature dependence, and the sensor is calibrated over simultaneous pressure and temperature sweeps (Fig. 7). A pressure accuracy of 0.17 mmHg is achieved.

D. Ex vivo porcine eye experiment

Before implantation, the silicone chamber and flexible tube are filled with saline, as bubbles may distort the sensed pressure. Post-implantation, a syringe is used to puncture the silicone chamber to flush any bubbles in the line that may have appeared from handling the tube during implantation.

The porcine eye is vitrectomized using a Stellaris PC vitrector (Bausch and Lomb, Inc.) using a standard 3-port technique and 23 gauge instrumentation, with the infusion line placed inferiorly. The vitrector is then removed and the 23-gauge flexible tube is inserted through this port. IOP is modified by adjusting the hydrostatic pressure of the infusion line using the IOP setting on the machine (Fig. 8a-c). The IOP in the porcine eye was swept between 5 and 34 mmHg in steps of 1 mmHg every 30 seconds. A small mismatch in the *ex vivo* data at IOP levels below 10 mmHg (Fig. 8d) are not attributed to implant measurement error, because the implant shows ideal performance in the same regime in a water column benchtop test (Fig. 8e). Thus, we conclude that the mismatch is attributed to reference error by the vitrector.

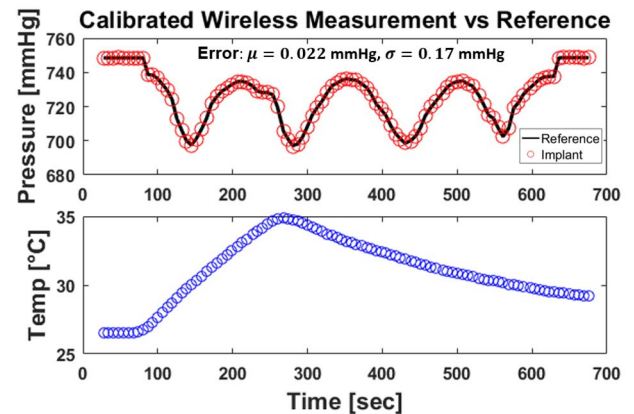


Figure 7: Calibrated wireless pressure sensor data versus a reference pressure. The interpreted values match the reference closely over simultaneous pressure and temperature variation. Plotted values are subsampled for visual clarity. The true sampling period is 1 sec.

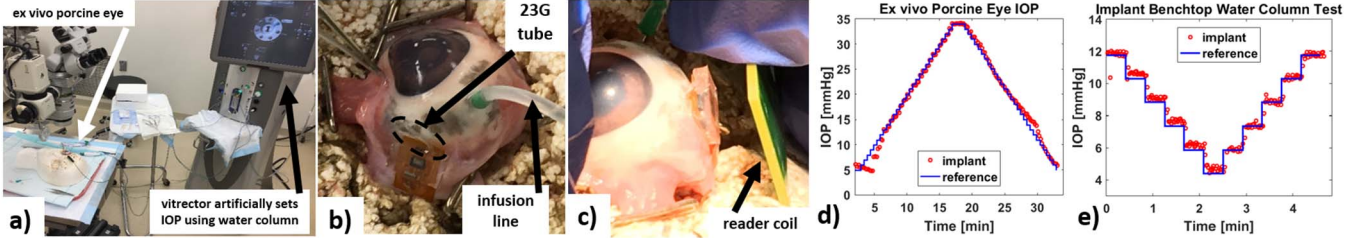


TABLE 1: PERFORMANCE COMPARISON

Metric	This work	JSSC'17 [10]	ISSCC'15 [11]	TCAS-I'13 [5]	JSSC'11 [12]
Technology	65nm	180nm	350nm	180nm	130nm
Full System (Wireless)	Yes	Yes	Yes	No	Yes
On-chip Integrated Coil (Power and Data)	Yes	No	No	No	No
Data Modulation	Backscatter	Backscatter	Backscatter	FSK	Backscatter
Power Harvesting Frequency	915 MHz	434 MHz	13.56 MHz	N/A	2.4 GHz
Power Harvesting Source	RF	MRC/Cavity Resonator	RF	Battery	RF
IOP drift	<0.5 mmHg for 120 days of saline tests across 30-37 °C	Not discussed	Not discussed	Not discussed	Not discussed
Temperature Offset Compensation	Yes	No	No	No	Yes
Pressure Sensitivity	0.17 mmHg	0.67 mmHg	0.027 mmHg	0.5 mmHg	0.9 mmHg
Long-term sensor reliability	Yes	No	No	No	No
Implant Packaging Technique	Parylene-on-oil	Parylene	Not discussed	Glass enclosure	Not discussed
Chip Area	2 mm x 1.2 mm	0.75 mm x 0.7 mm	2 mm x 1 mm	1.8 mm ²	1 mm x 0.7 mm
Power	9.7 μW	48.9 μW	1.2 mW	N/A	2.3 μW

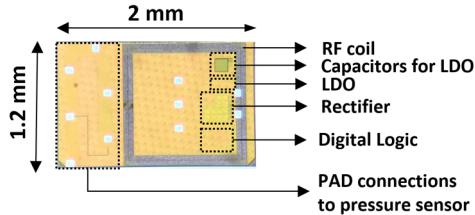


Figure 9: Die photo

IV. CONCLUSION

A wireless, implantable, low-drift intraocular pressure monitor is demonstrated. A chip was fabricated in TSMC 65nm CMOS, which receives RF power through an integrated on-chip coil and powers the IOP implant and transmits data via backscattering (Fig. 9). Total power consumption of the implant is 9.7 μ W, achieving a pressure sensitivity of 0.17 mmHg. We demonstrate <0.5 mmHg pressure offset drift for 4 months over a temperature range of 27-38 °C in saline tests (Table 1). Functionality and surgical implantation are validated in *ex vivo* porcine eye tests.

ACKNOWLEDGMENT

The authors thank Samson Chen (Caltech Nanofabrication Lab) for help with the wireless reader, Trevor Roper (Caltech MEMS Lab) for maintaining equipment, Cameron Sylber for help with longevity tests, and MOSIS for chip fabrication. This work was supported by the Rosen Bioengineering Center Pilot Grant, the Heritage Medical Research Institute, the L. K. Whittier Foundation, and an unrestricted departmental grant from Research to Prevent Blindness.

REFERENCES

- [1] Quigley et al., "The number of people with glaucoma worldwide in 2010 and 2020," *Brit. J. Ophthalmol.*, vol. 90, pp. 262–267, Mar. 2006.
- [2] Mansouri et al., Analysis of Continuous 24-Hour Intraocular Pressure Patterns in Glaucoma. *Investigative Ophthalmology & Visual Science*, 2012; 53(13), 8050–8056.
- [3] Yu et al., Chronically implanted pressure sensors: Challenges and state of the field. *Sensors*, 2014, 14(11), 20620-20644.
- [4] Downs et al., 24-Hour IOP Telemetry in the Nonhuman Primate: Implant System Performance and Initial Characterization of IOP at Multiple Timescales. *Investigative Ophthalmology & Visual Science*, 2011; 52(10), 7365–7375.
- [5] Ghaed et al., "Circuits for a Cubic-Millimeter Energy-Autonomous Wireless Intraocular Pressure Monitor," in *IEEE Transactions on Circuits and Systems I: Regular Papers*, vol. 60, no. 12, pp. 3152-3162, Dec. 2013.
- [6] Shapero et al., Parylene-on-oil packaging for long-term implantable pressure sensors. *Biomedical Microdevices*, 2016, 18(4), 1-10.
- [7] Agarwal et al., "A 4 μ W, ADPLL-based implantable amperometric biosensor in 65nm CMOS," 2017 Symposium on VLSI Circuits, Kyoto, 2017, pp. C108-C109.
- [8] Shapero et al., "Parylene-oil-encapsulated low-drift implantable pressure sensors," 2018 IEEE 31st International Conference on Micro Electro Mechanical Systems (MEMS), Belfast, 2018, (in press)
- [9] Ho et al., "Midfield Wireless Powering for Implantable Systems," in *Proceedings of the IEEE*, vol. 101, no. 6, pp. 1369-1378, June 2013.
- [10] Bhamra et al., "A Subcubic Millimeter Wireless Implantable Intraocular Pressure Monitor Microsystem," in *IEEE Transactions on Biomedical Circuits and Systems*, vol. PP, no. 99, pp. 1-12, Nov. 2017.
- [11] Donida et al., "A Circadian and Cardiac Intraocular Pressure Sensor for Smart Implantable Lens," in *IEEE Transactions on Biomedical Circuits and Systems*, vol. 9, no. 6, pp. 777-789, Dec. 2015.
- [12] Shih et al., "A 2.3 μ W Wireless Intraocular Pressure/Temperature Monitor," in *IEEE Journal of Solid-State Circuits*, vol. 46, no. 11, pp. 2592-2601, Nov. 2011.